JOURNAL OF GEOPHYSICAL RESEARCH, VOL. 115, D16302, doi:10.1029/2009JD013715, 2010

Variations in surface ozone at Nainital: A high-altitude site in the central Himalayas

Rajesh Kumar,[1] Manish Naja,[1] S. Venkataramani,[2] and O. Wild[3]

Received 15 December 2009; revised 26 March 2010; accepted 7 April 2010; published 17 August 2010.

[1] Surface ozone measurements have been made for the first time at Nainital (29.37°N, 79.45°E, 1958 m amsl), a high-altitude site in the central Himalayas, between October 2006 and December 2008. Diurnal variations in ozone do not show the daytime photochemical build-up typical of urban or rural sites. The seasonal variation shows a distinct ozone maximum in late spring (May; 67.2 ± 14.2 ppbv) with values sometimes exceeding 100 ppbv and a minimum in the summer/monsoon season (August; 24.9 ± 8.4 ppbv). Springtime ozone values in the central Himalayas are significantly higher than those at another high-altitude site (Mt. Abu) in the western part of India. Seasonal variations in ozone and the processes responsible for the springtime peak are studied using meteorological parameters, insolation, spatial and temporal classifications of air mass trajectories, fire counts, and simulations with a chemical transport model. Net ozone production over the Northern Indian Subcontinent in regionally polluted air masses is estimated to be 3.2 ppbv/day in spring but no clear build-up is seen at other times of year. Annual average ozone values in regionally polluted air masses (47.1 ± 16.7 ppbv) and on high insolation days (46.8 ± 17.3 ppbv) are similar. Background ozone levels are estimated to be 30–35 ppbv. Regional pollution is shown to have maximum contribution (16.5 ppbv) to ozone levels during May–June and is about 7 ppbv on an annual basis, while the contribution of long-range transport is greatest during January–March (8–11 ppbv). The modeled stratospheric ozone contribution is 2–16 ppbv. Both the trajectory analysis and the model suggest that the stratospheric contribution is 4–6 ppbv greater than the contribution from regional pollution. Differences in the seasonal variation of ozone over high-altitude sites in the central Himalayas (Nainital) and western India (Mt. Abu) suggest diverse regional emission sources in India and highlight the large spatial and temporal variability in ozone over the Indian region.

Citation: Kumar, R., M. Naja, S. Venkataramani, and O. Wild (2010), Variations in surface ozone at Nainital: A high-altitude site in the central Himalayas, *J. Geophys. Res.*, *115*, D16302, doi:10.1029/2009JD013715.

1. Introduction

[2] Ozone is recognized as an important gas responsible for changes in air quality and global climate. It is a major precursor of highly reactive hydroxyl (OH) radicals, which determine the lifetime of many gases in the atmosphere. Higher levels of ozone in the boundary layer lead to serious health problems [e.g., *Desqueyroux et al.*, 2002], can damage natural ecosystems and reduce crop yields [e.g., *Mauzerall and Wang*, 2001; *Oksanen and Holopainen*, 2001]. Such detrimental impacts from high ozone have been seen in different regions, particularly in some Asian regions where higher ozone levels and a positive trend in ozone have been reported [e.g., *Dickerson et al.*, 2007; *Tanimoto*, 2009]. *Ding et al.* [2008] have reported a strong positive trend of ~2% per year from 1995 to 2005 over Beijing. Significant increases (about 0.5–0.9 ppbv per year) in surface ozone over Southern China [*Wang et al.*, 2009] and increases in the frequency of extreme values (monthly highest 5% of ozone concentrations) over Eastern China [*Xu et al.*, 2008] since early 1990s have also been reported recently. In addition, emissions of key ozone precursors are strongly increasing in Asia, while they are now steady or decreasing in most parts of Europe and the United States [*Streets and Waldhoff*, 2000; *Akimoto*, 2003; *Naja et al.*, 2003a; *Ohara et al.*, 2007].

[3] Generally, ozone is observed to be higher in spring and summer at many measurement sites over the globe. Some high-altitude sites (e.g., Mt. Fuji, 35.35°N, 138.73°E, 3776 m amsl and Mauna Loa, 19.5°N, 155.6°W, 3397 m amsl) show a springtime maximum value which is largely explained on the basis of downward transport of ozone-rich air from higher altitudes [e.g., *Tsutsumi et al.*, 1994; *Oltmans et al.*, 2006] while there have been different explanations of the summertime maximum value observed at Waliguan (36.28°N, 100.9°E, 3810 m amsl) [*Tang et al.*, 1995]. *Zhu et al.* [2004] proposed that transport of polluted air masses from eastern/

[1] Aryabhatta Research Institute of Observational Sciences, Nainital, India.
[2] Physical Research Laboratory, Navrangpura, Ahmedabad, India.
[3] Lancaster Environment Centre, Lancaster University, Lancaster, UK.

0148-0227/10/2009JD013715

central China and central/south Asia is responsible for the summertime maximum at Waliguan while other studies [e.g., *Ma et al.*, 2005; *Zheng et al.*, 2005; *Ding and Wang*, 2006] have suggested that subsidence of upper tropospheric/stratospheric air over Tibetan plateau brings ozone-rich air to the surface there in summer. Springtime maximum ozone levels observed at Arosa (46.77°N, 9.47°E, 1840 m amsl) and Mt. Happo (36.70°N, 137.80°E, 1850 m amsl) have been attributed mostly to regional pollution [*Staehelin et al.*, 1994; *Pochanart et al.*, 2001; *Tanimoto*, 2009]. At low altitude sites, high summertime ozone levels are generally attributed to more intense in situ photochemical production [e.g., *Logan*, 1985; *Solberg et al.*, 2008].

[4] In contrast, available observations [*Lal et al.*, 2000; *Naja and Lal.*, 2002; *Nair et al.*, 2002] and modeling studies [*Beig et al.*, 2007; *Mittal et al.*, 2007; *Engardt*, 2008] for the western and southern Indian region show higher ozone levels during late autumn and winter extending until March. Such variations over India are due to higher levels of precursors and the availability of sufficient solar radiation even in winter. Generally, the summer period over most of the Indian region is dominated by the monsoon, with cloudy conditions and the arrival of pristine air masses from the Arabian Sea, Bay of Bengal and Indian Ocean. Observations at Delhi, on the Indo-Gangetic Plain, show maxima in spring and autumn, when levels of pollutants are high and solar radiation over this region is intense [*Jain et al.*, 2005]. It is to be noted that surface ozone observations with a complete seasonal cycle are not available over the northern Indian region except at New Delhi.

[5] The observation site Nainital in the central Himalayas is located just north of the Indo-Gangetic Plain (IGP). The IGP is a homogeneous plain lying between the foothills of the Himalayas in the North, the Deccan Plateau in the south, the Pakistan provinces of Sind and Punjab to the west and the Brahmaputra river valley to the east. It is one of the most densely populated regions in the world, accommodating an average of 250–1000 persons per km^2 (CIESIN; http://sedac.ciesin.columbia.edu/gpw) and encompassing major Indian industrialized cities such as Delhi, Kanpur, Lucknow, Patna, and Kolkata with populations in the range of 1.5–13 million (http://www.censusindia.gov.in). In addition to different industries, extensive agricultural activities in this region lead to the emission of pollutants through burning of crop residues. Air masses from this polluted IGP region influence most of India, including marine regions, throughout the year, particularly during late autumn and early winter [*Niranjan et al.*, 2006], and the influence may extend as far as the Pacific during spring.

[6] Satellite-based observations have shown high levels of total tropospheric ozone [*Fishman et al.*, 2003] and high aerosol optical depth [*Di Girolamo et al.*, 2004; *Jethva et al.*, 2005] over the IGP. Surface observations of aerosols also show elevated levels from this region [e.g., *Tripathi et al.*, 2005]. However, in situ observations of surface ozone and precursors are very sparse in this region and are available only at Delhi (28.35°N, 77.12°E, 220 m amsl) [*Aneja et al.*, 2001; *Jain et al.*, 2005]. In the eastern Himalayas, surface ozone observations have been reported at an urban site (Kathmandu, Nepal, 27.75°N, 85.15°E, ~1300 m amsl) [*Pudasainee et al.*, 2006; *Panday and Prinn*, 2009]. The presence of daytime photochemical build-up in ozone diurnal variations at Delhi and Kathmandu suggests that data from these observation sites are influenced by local emissions and are representative of a small region only.

[7] In light of these conditions, we expect that observations at Nainital will be more regionally representative of Northern India, including the IGP region. In this perspective, we report here for the first time surface ozone observations at this high-altitude site. The manuscript begins with a brief overview of the observation site and general meteorology in section 2. Details of the instruments used for in situ measurements, trajectory calculations and chemical transport model (CTM) are presented in section 3. Diurnal and seasonal variations in ozone at Nainital together with different approaches employed to explain these variations and comparison of observations with model simulations are discussed in section 4.

2. Observation Site and General Meteorology

[8] The observation site is located on a mountaintop called Manora Peak (29.37°N, 79.45°E, 1958 m amsl) in Nainital (hereafter, the observation site is referred to as Nainital). Sharply peaking mountains are located to the north and east of the observation site (auxiliary material Figure S1).[1] Mountains with altitudes less than 1000 m are located to the south and west. The main town of Nainital is about 2 km away from the observational site toward the north. There is no industry in Nainital and the population is about 0.4 million. The nearby cities of Haldwani (423 m amsl) and Rudrapur (209 m amsl), which are 20–40 km from this site, have some small-scale industries and are located to the south, and the nearest major city, Delhi, is about 225 km away to the southwest.

[9] Figure 1 shows the origin of air masses influencing the site for winter (January), late spring (May), summer/monsoon (June) and early autumn (September) based on backward air mass trajectory calculations. These trajectory patterns are derived using 10-day backward trajectories at Nainital for 2007–2008 in the respective months and these patterns are found to be similar over the last six years (2003–2008) (auxiliary material Figure S2). Details of the trajectory calculations are given in section 3.2. Note that air masses at this site do not arrive from the northeastern sector in any season because of high mountains in that direction. Generally, the wind pattern is westerly/northwesterly in winter and changes gradually to southwesterly during June–July, while in May and September air masses circulate mostly over the Northern Indian region. The trajectory patterns change again from southwesterly to westerly/northwesterly during October–November (not shown), and these continue until March–April. Such changes in wind pattern are observed every year [*Asnani*, 2005]. The topography around the observation site and the general meteorology prevailing during different seasons have been discussed in detail by *Sagar et al.* [2004] and *Pant et al.* [2006].

3. Observation Techniques and Data Analysis

3.1. Ozone, CO, CH_4, and Meteorological Parameters

[10] Continuous observations of surface ozone have been made since October 2006 using an ozone analyzer

[1] Auxiliary materials are available in the HTML. doi:10.1029/2009JD013715.

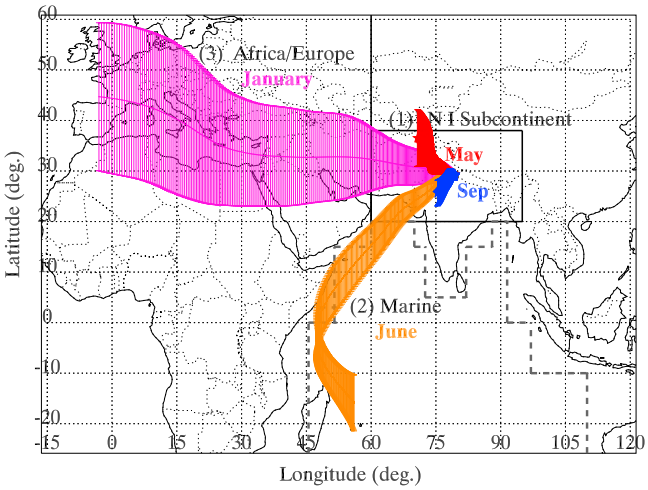

Figure 1. Most probable back-air trajectories (10 days) at Nainital showing westerly winds during winter (January) and southwesterlies during summer/monsoon (June). Late spring (May) and early autumn (September) are the change over periods and winds mostly circulate over the Indian subcontinent. These average patterns of back-air trajectories are determined using daily trajectories in respective months of the years 2007 and 2008. Regional classification of Northern Indian (N I) Subcontinent, marine, and Africa/Europe is also shown.

(Environment S.A., France; Model O_3 41 M) that is based on the well-known technique of UV absorption. The analyzer aspirates the air from a height of about 5 m above the ground level through a Teflon tube with a flow rate of about 1 L per minute. The minimum detection limit of the analyzer is about 1 ppbv. The response time of this system is 10 s and absolute accuracy is reported to be about 5% [*Kleinman et al.*, 1994]. Checks of its calibration and inter comparison with another ozone instrument (Thermo Electron Corporation, USA, Model 49*i*) are performed regularly. Further details of the analyzer can be seen elsewhere [*Naja and Lal*, 2002]. Average data over 15 min intervals are stored and used in this study.

[11] Air samples were collected over five months (February–June 2007) with a frequency of three samples per week (Monday, Wednesday and Friday at 1430 h) in pre-evacuated glass bottles at a pressure of 1.6 bar using a metal bellows pump for the analysis of CO and CH_4. These air samples are then analyzed with the help of a gas chromatograph equipped with a Flame Ionization Detector (FID) together with a methanizer (heated Ni catalyst) at Physical Research Laboratory, Ahmedabad. Further details regarding the calibration and accuracy for gas chromatograph can be seen in the work of *Lal et al.* [2000]. An automatic weather station (Campbell Scientific Inc., Canada and Dynalab, India) has been used for the observations of meteorological parameters with a time resolution of 20 min. Downward solar radiation fluxes from NCEP reanalysis data, available four times daily (00, 06, 12, and 18 GMT) on a T62 Gaussian grid (1.9° resolution), are also used, along with monthly average rainfall data from TRMM and other rainfall estimates (3B43 V6).

3.2. Back-Air Trajectory and Classifications

[12] The Meteorological Data Explorer (METEX) model [*Zeng et al.*, 2003] is used for backward trajectory calculations. The model was developed at the National Institute for Environmental Studies (NIES), Japan and Global Environmental Forum, Japan. NCEP reanalysis data available at a spatial resolution of 2.5° and temporal resolution of 6 h are used in the trajectory calculations. Clusters of five trajectories, 4 trajectories at the corners of a 0.5° × 0.5° grid around Nainital and one centered on Nainital, are generated at an altitude of 2200 m above sea level. Such clusters of five 10-day backward trajectories are generated each day at 00, 06, 12, and 18 GMT. Sometimes the five trajectories are not coherent and these trajectories are excluded from the analysis following the filtering criterion discussed in detail by *Naja et al.* [2003a].

[13] Three regions are defined to allow a spatial classification of the trajectories (see Figure 1): (1) the region from 20°N to 38°N and from 60°E to 95°E is designated as the Northern Indian Subcontinent; (2) the Arabian Sea, Bay of Bengal and Indian Ocean are designated as the marine region and (3) the region from 15°W to 60°E and from 35°S to 70°N (excluding the marine region near the boundary of African continent) is designated as Africa/Europe. However, it should be noted that 85–90% of the air masses arriving at Nainital from Africa/Europe region originate from Northern Africa and Southern Europe. These three regions represent the effects of regional pollution from the Northern Indian Subcontinent, marine air masses and long-range transport on ozone levels at Nainital, respectively.

[14] The residence times of air masses in these three regions are also determined and used in their classification. Average residence times are estimated each day over the Northern Indian Subcontinent, marine and Africa/Europe at four times (00, 06, 12, and 18 GMT), based on the nearest whole number of days an air mass spends over the respective region. Ozone observations within ± 30 min of the trajectory simulation time each day at Nainital are averaged and tagged with the corresponding residence times of the air masses and are used for further analysis. The altitude information of the air masses is used to filter out the local and higher altitude effects. Additional details on air mass categorization along with ozone values are provided in section 4.4.

3.3. Fire Counts

[15] Fire count data are obtained from the Advanced Along Track Scanning Radiometer (AATSR) using data from algorithm 1, which identifies a hot spot if the temperature is greater than 312°K in the 3.7 micron band. The spatial resolution of the AATSR instrument is 1 km. Other space-borne systems that provide information about fires are the Advanced Very High Resolution Radiometer (AVHRR) and Moderate Resolution Imaging Spectroradiometer (MODIS). Data from both AVHRR and MODIS suffer from contamination by solar radiation during daytime which may lead to over-estimation of fires [*Kaufman et al.*, 1998, and references therein]. However, the problem of contamination is less for MODIS data [*Kaufman et al.*, 1998]. In contrast, AATSR by virtue of its nighttime operation minimizes solar reflection contamination (http://dup.esrin.esa.int/ionia/wfa/algorithm.asp) but may underestimate fire counts by

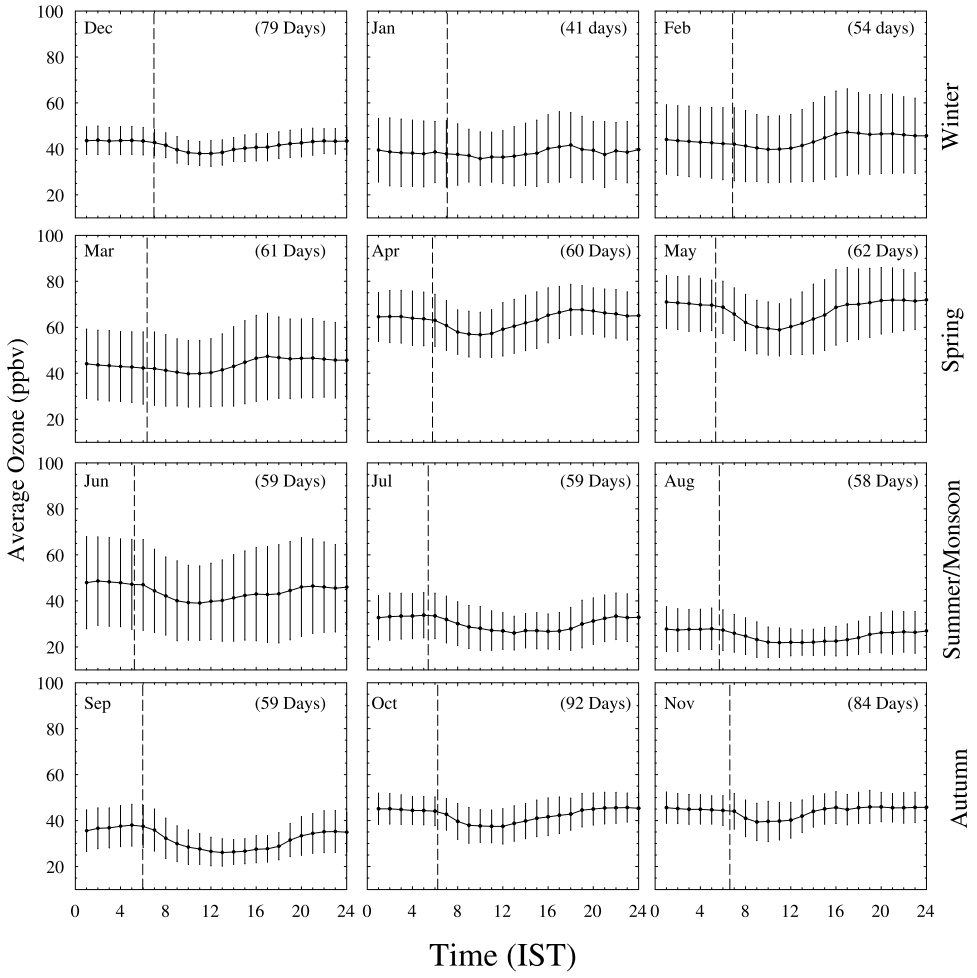

Figure 2. Diurnal variations in hourly averaged ozone mixing ratios at Nainital in different months for the period of October 2006 to December 2008. Indian Standard Time (IST) is 5.5 h ahead of Greenwich Mean Time (GMT). The average sunrise time in different months during the entire observation period is shown by a dashed vertical line and the number of observation days in each month is shown in parentheses.

missing short-term daytime fires which can be an important source of uncertainty in the quantification of fire emissions. In the present study, we use fire counts only to represent the seasonal variation in fire activity over the Northern Indian subcontinent.

3.4. Model Analysis

[16] This study uses results from the Frontier Research System for Global Change version of the University of California, Irvine chemical transport model (FRSGC/UCI CTM) [*Wild and Prather*, 2000]. The model is driven with 3-h meteorological data from the European Centre for Medium-Range Weather Forecasts (ECMWF) and is run at T42 resolution (2.8° × 2.8°) with the configuration described by *Wild et al.* [2004]. The model uses the ASAD modular chemistry package [*Carver et al.*, 1997] and anthropogenic emissions are based on IIASA scenarios for 2000 constructed for an earlier model intercomparison [*Stevenson et al.*, 2006]. Monthly mean emissions from biomass burning are based on satellite-derived distributions from *van der Werf et al.* [2003] averaged over the 1997–2002 time period. Results from these simulations were used in model intercomparisons organized for the Hemispheric Transport of Air Pollution (HTAP) studies described by *Fiore et al.* [2009].

4. Results

4.1. Diurnal Variations in Ozone

[17] Figure 2 depicts the average diurnal variations of ozone in different months, representing the four seasons, namely winter (DJF), spring (MAM), summer/monsoon (JJA) and autumn (SON) for the period of October 2006 to December 2008. These diurnal variations at Nainital do not show the signature of daytime photochemical build-up in ozone typical of most urban or rural sites. Average ozone values show a slight decrease immediately after sunrise that is followed by a systematic increase in the evening and thus lower mixing ratios are common during daytime at the site. Such diurnal patterns in ozone with lower daytime levels are generally observed at cleaner higher altitude sites that are reasonably away from emission sources (e.g., Mauna

Table 1. Monthly Average Ozone, Along With One Sigma Deviation, Maximum, Minimum, and Number of Observations From October 2006 to December 2008[a]

Month	Ozone[b] (ppbv)	Ozone Minimum (ppbv)	Ozone Maximum (ppbv)	Ozone Count	CO[b] (ppbv)	CH_4[b] (ppmv)	Air Samples Count
January	37.3 ± 14.8	5	66	3437	-	-	-
February	43.8 ± 16.8	8	87	4525	193.6 ± 81.5	1.84 ± 0.03	8
March	56.6 ± 11.4	26	92	5493	272.1 ± 164.0	1.89 ± 0.08	10
April	63.1 ± 11.7	35	100	5587	267.4 ± 102.3	1.87 ± 0.05	12
May	67.2 ± 14.2	30	113	5555	333.6 ± 297.1	1.87 ± 0.10	11
June	44.0 ± 19.5	11	107	5438	315.6 ± 84.3	1.93 ± 0.01	3
July	30.3 ± 9.9	10	62	5450	-	-	-
August	24.9 ± 8.4	9	62	5186	-	-	-
September	32.0 ± 9.1	13	61	5350	-	-	-
October	42.4 ± 7.9	14	78	8420	-	-	-
November	43.9 ± 7.6	26	88	7464	-	-	-
December	41.6 ± 6.3	26	64	6782	-	-	-

[a]Maximum, minimum, and count indicate the maximum, minimum, and total counts for 15 min averaged ozone measurements. Monthly average and one sigma deviation for CO and CH_4 are also shown along with the number of air samples.
[b]Mean ± 1 Sigma.

Loa, 19.5°N, 155.6°W, 3397 m amsl, Mt. Fuji, 35.35°N, 138.73°E, 3776 m amsl and Mt. Abu, 24.6°N, 72.7°E, 1680 m amsl) [*Oltmans and Levy*, 1994; *Tsutsumi et al.*, 1994; *Naja et al.*, 2003b]. However, some high-altitude sites (e.g., Niwot Ridge, 40°N, 106°W, 3000 m amsl) showing daytime photochemical build-up in ozone may be influenced by emissions from nearby sources [*Oltmans and Levy*, 1994].

[18] Table 1 shows monthly average values of CO and CH_4 determined from the air samples. It is evident that levels of CO (<334 ppbv) and CH_4 (<1.93 ppmv) at Nainital are lower than those reported in earlier studies at Ahmedabad (urban; CO > 3000 ppbv and CH_4 < 2 ppmv) and Gadanki (rural; CO > 600 ppbv and CH_4 < 2 ppmv) sites in India [*Lal et al.*, 2000; *Naja and Lal*, 2002], although it should be noted that these observations were made during the mid-1990s. The levels of other ozone precursor gases are also anticipated to be lower at Nainital. Hence, the absence of daytime build-up in ozone diurnal variations together with moderate to lower levels of precursors suggest that the present site is reasonably away from emission sources and local photochemistry contributes little to ozone variations at Nainital.

4.2. Seasonal Variations in Ozone

[19] Figure 3 shows hourly average ozone values and monthly statistics of ozone mixing ratios at Nainital during October 2006 to December 2008. A systematic increase in ozone is observed from January to early June and afterward its levels show a dramatic decrease with lower mixing ratios continuing until August. Ozone then increases and shows a secondary maximum during October–November. Monthly statistics of ozone, CO and CH_4 levels at Nainital are shown in Table 1. Ozone exhibits a clear spring maximum with highest monthly mean values in May (67.2 ± 14.2 ppbv) and a summer/monsoon minimum with lowest values in August (24.9 ± 8.4 ppbv). CO levels are also highest in May but CH_4 does not show any significant variation.

[20] Figure 3 also shows the monthly variation (1993–2000) in ozone at Mt. Abu (24.6°N, 72.7°E, 1680 m amsl), a high-altitude site in Western India [*Naja et al.*, 2003b] (see location in auxiliary material Figure S1). In contrast to Nainital, ozone mixing ratios show a systematic decrease from February to June but are reasonably similar from August onwards. Interestingly, ozone levels are 62–73% higher over the central Himalayas in April and May than over Western India. Average ozone values at Mt. Abu and Nainital on the other hand fall within 20% of each other from August to February. There is not much difference in the altitude of Nainital and Mt. Abu, but the sites are representative of different regions, namely of Northern India (including the IGP) and western India respectively (auxiliary material Figure S1). Mt. Abu is close to the Arabian Sea and therefore arrival of pristine marine air masses leads to a

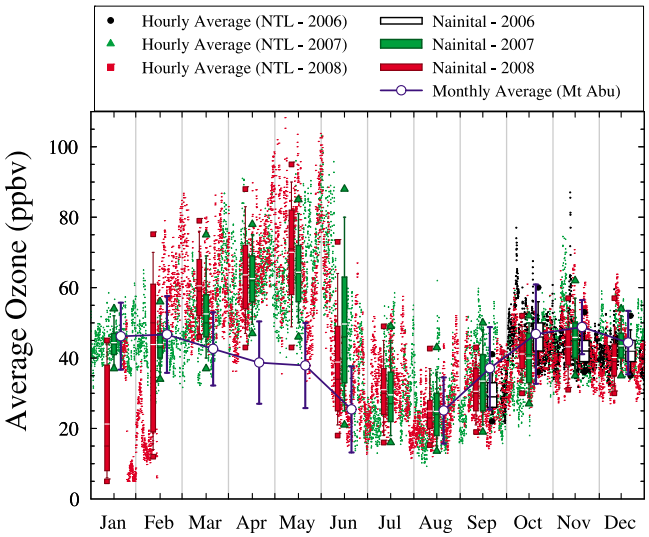

Figure 3. Variations in ozone mixing ratios from October 2006 to December 2008 at Nainital. In box plots, the solid white and black lines inside the box represent the mean and median of the data respectively. The lower and upper edges of boxes represent the 25th and 75th percentiles. The whiskers below and above are 10th and 90th percentiles and the outliers in the box plot show 5th and 95th percentiles in 15 min average ozone data. Monthly average ozone values (1993–2000) at another high-altitude site in western India, Mt. Abu (24.6°N, 72.7°E, 1680 m amsl) are also shown for a comparison.

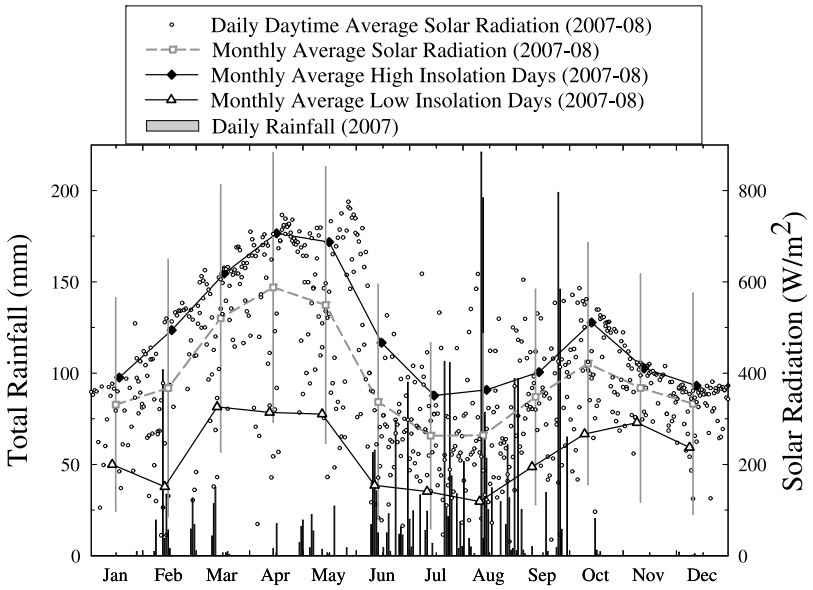

Figure 4. Variations in daily daytime (0700–1700 h) average solar radiation, monthly average solar radiation, and monthly average solar radiation during high and low insolation days from January 2007 to December 2008. Solar radiation data are not available for January 2007. Daily total rainfall data during 2007 is also shown.

decrease in ozone levels during late spring [*Naja et al.*, 2003b].

[21] To explain the variations observed at Nainital, we apply a range of different approaches, examining the association of observed ozone with (1) solar irradiance, (2) air masses influenced by regional emissions from the Northern Indian Subcontinent, (3) air masses from marine and distant continental regions, and (4) downward transport from higher altitudes. Possible roles of fire activities and rainfall in influencing the ozone seasonal variations are also discussed. The influence of variations in solar irradiance is considered by characterizing ozone levels on days with high and low insolation (section 4.3). The residence times of air masses arriving along the calculated trajectories are estimated to distinguish the contribution of regional pollution from the Northern Indian Subcontinent, the influence of marine air masses and long-range transport from Africa/Europe (section 4.4). An attempt is made to explore the influence of downward transport from higher altitudes in section 4.5.

4.3. Ozone, Solar Radiation, Rainfall, and Biomass Burning

[22] Seasonal variation in daily daytime average (0700–1700 h Indian Standard Time (IST), 5.5 h ahead of GMT) solar radiation, monthly average solar radiation, monthly average solar radiation during "high and low insolation days" and daily total rainfall during 2007 are shown in Figure 4. High and low insolation days are defined as 50% and 25% of days in the respective months with the highest and lowest solar radiation respectively and represent conditions with the most and least intense photochemistry. The solar radiation data are not available during October 2006 to January 2007 due to a technical problem with the sensor. In order to compensate for the loss of data during this period, NCEP reanalysis downward solar radiation flux data from 06 and 12 GMT are used to calculate daily average daytime solar radiation at a location (29.52°N, 80.62°E) nearest to Nainital (termed as NCEP solar radiation at Nainital hereafter). Since NCEP reanalysis downward solar radiation flux do not incorporate any information from observations and are solely derived from the model [*Kalnay et al.*, 1996], this product needs to be validated against observations before it can be used for any scientific analysis. We have therefore compared NCEP solar radiation at Nainital with the observed solar radiation at Nainital and found a positive correlation ($r^2 = 0.87$) between the two data sets during February 2007 to December 2008 (auxiliary material Figure S3a).

[23] In general, the seasonal variations in solar radiation are in good agreement with the seasonal variations in ozone. A systematic increase in both solar radiation and ozone is seen from January to May, just prior to the arrival of the southwest monsoon in June. The arrival of the monsoon is responsible for the abrupt fall in solar radiation and ozone mixing ratios in June. It is also evident that rainfall is more frequent during June–September (about 80% of the annual rainfall) than in other months. Rainfall during late January to mid February 2008 and snowfall during mid February coincided with a dramatic fall in ozone values of up to 4–5 ppbv (Figure 3). The end of monsoon during September leads to a decrease in rainfall and an increase in solar radiation and this coincides with an increase in ozone. Similar seasonal variations in solar radiation and rainfall are also seen over the Northern Indian Subcontinent (auxiliary material Figure S4).

4.3.1. Biomass Burning

[24] Biomass burning plays an important role in atmospheric chemistry through emission of trace gases and particulate matter into the atmosphere which may lead to ozone production during favorable meteorological conditions. Figure 5 shows seasonal variations in daily and monthly total fire

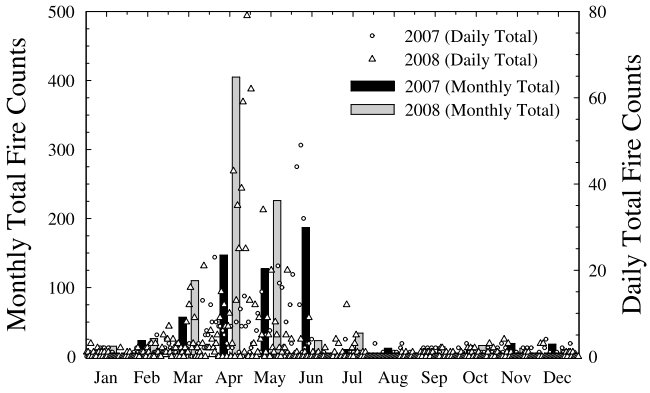

Figure 5. Daily and monthly total fire counts over the Northern Indian Subcontinent from January 2007 to December 2008. Labels on the left are for monthly total fire counts, and labels on the right are for daily total fire counts.

counts during 2007 and 2008 over the Northern Indian Subcontinent. In general, an increase in fire counts is seen from January to May–June (with exceptionally high fire count for a few days in April 2008) and is similar to the variations in average ozone (Figure 3). Very few fire events are seen after mid June largely due to rainfall. There are generally less than 5 fire counts on a single day until February, while fire counts exceed 40 on many occasions in April, May and June. Qualitatively, more fire events in June 2007 and May 2008 are correlated with higher monthly mean ozone values in respective months. Here, it is suggested that the greatest influence of biomass burning on ozone levels could be in spring at Nainital. There is a need to make more quantitative assessment of the contribution from fires; however it is not being pursued here.

4.3.2. Ozone on High and Low Insolation Days

[25] Figure 6 shows variations in monthly average ozone associated with high and low insolation days for the period of October 2006 to December 2008. Annual average ozone on high insolation days is estimated to be 46.8 ± 17.3 ppbv whereas that on low insolation days is 39.9 ± 14.2 ppbv. To test the robustness of our classification, we perform a sensitivity analysis using a threshold of 40% days with higher solar radiation and find that the average ozone is almost unaffected (46.9 ± 17.7 ppbv).

[26] Figure 6 also shows the variation in the difference between ozone on high and low insolation days, a marker of the build-up in ozone due to photochemistry. The largest ozone build-up (~16.5 ppbv) is seen during May–June while the lowest build-up (<1 ppbv) is seen during July and August, when the site experiences extensive rainfall. As noted earlier, the absence of a daytime ozone increase at Nainital (Figure 2) suggests that in situ photochemical ozone production close to the site plays a negligible role. Therefore, the observed photochemical build-up is driven by net photochemical ozone production over the Northern Indian Subcontinent region. This is investigated further by comparing the calculated daily daytime average solar radiation data from NCEP over the defined Northern Indian Subcontinent region with the observed solar radiation at Nainital. Since these are positively correlated ($r^2 = 0.76$) (auxiliary material Figure S3b), we suggest that the observed seasonal build-up in ozone at Nainital is due to regional sources within the Northern Indian Subcontinent and not due to local in situ photochemistry at Nainital.

4.4. Backward Trajectory Analysis

4.4.1. Correlation Between Residence Time and Ozone

[27] Figure 7 shows the correlation between air mass residence time over the Northern Indian Subcontinent and the associated ozone mixing ratios (as discussed in section 3.2) at Nainital. Here we define the spring season as 1 March to 10 June, and summer/monsoon as 11 June to 31 August, to account for the start of the monsoon. The first 10 days of June (1–10 June) were very sunny (e.g., Solar Radiation = 615.9 ± 131.1 W/m^2, RH = 50.5 ± 16.1% during 2007) and thereafter, i.e., 11 June onward, rainfall started. In this analysis, residence times over the Northern Indian Subcontinent region are considered only for trajectories with median altitudes less than 4000 m within this region (see Figure 1) to allow greater contribution from regional sources and limit the influence of downward transport from higher altitudes. Further, ozone data from low insolation days has not been considered here due to reduced net photochemical ozone production under cloudy conditions.

[28] Ozone mixing ratios at Nainital in spring are seen to increase at a rate of 3.2 ppbv per day until a residence time of 5 or 6 days is reached over the Northern Indian Subcontinent. This increase is due to the accumulation of ozone and its precursors over this region during the residence period of 5–6 days. The availability of sufficient solar radiation induces ozone formation through the photo-oxidation of the accumulated precursors and solar radiation is highest in spring over this region (see Figure 4). The build-up in ozone appears to saturate for residence periods greater than 6 days during spring. Such features have also been observed over central Europe [e.g., *Pochanart et al.*, 2001; *Naja et al.*, 2003a]. Ozone mixing ratios do not change significantly with residence time of air masses in other seasons, although they show a slight increase during winter (0.3 ppbv per day) and autumn

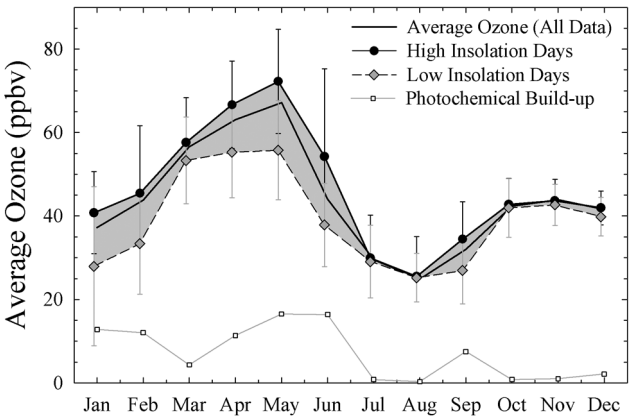

Figure 6. Monthly variations in all ozone data and in ozone associated with high and low insolation days during the period October 2006 to December 2008. The vertical bars represent one sigma variations in the corresponding averages. Photochemical build-up is shown by the difference between the average ozone values in high and low insolation days.

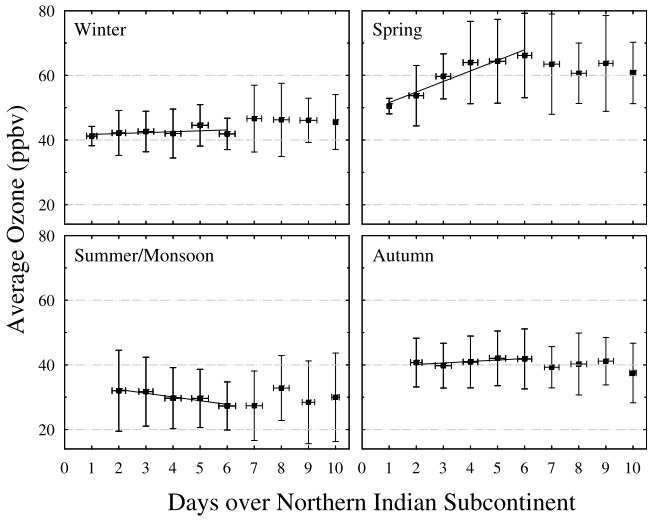

Figure 7. Changes in ozone mixing ratios at Nainital with respect to increase in residence time over the Northern Indian Subcontinent in winter, spring, summer/monsoon, and autumn during October 2006 to December 2008. Vertical bars show one sigma variation in average ozone mixing ratios and horizontal bars show one sigma variation in residence time over the Northern Indian Subcontinent.

(0.45 ppbv per day) and a small decrease during summer/monsoon (−1.1 ppbv per day). The washout of pollutants by rainfall may be responsible for the decrease during the monsoon, and the lower solar radiation over the Northern Indian Subcontinent in winter and autumn might contribute to slower net photochemical ozone formation.

[29] *Pochanart et al.* [2001] presented a simple and effective approach to estimate regional background ozone from the correlation between residence time of air masses and ozone mixing ratios, and this has been used successfully on long-term ozonesonde observations over Europe by *Naja et al.* [2003a]. A similar approach is used here to derive regional background ozone for the Northern Indian subcontinent. The correlation between the residence time of air masses and ozone mixing ratios is linearly extrapolated from six days back to zero, as discussed by *Pochanart et al.* [2001] to estimate the ozone in air masses entering the Northern Indian Subcontinent region. The linear regression employed in the derivation of regional background ozone introduces some uncertainty given the nonlinearity of ozone production [*Lin et al.*, 1988], but *Pochanart et al.* [2001] showed that the use of nonlinear (polynomial regression) extrapolation techniques do not provide significantly different results compared to those obtained with linear regression. Based on this approach, regional background ozone values are estimated to be 41.4 ± 2.9 ppbv in winter, 48.3 ± 5.0 ppbv in spring, 34.7 ± 2.8 ppbv in summer/monsoon and 39.2 ± 2.9 ppbv in autumn where the uncertainty here reflects the 95% confidence limit in the estimates.

4.4.2. Variations of Ozone in Different Air Masses

[30] Considering the correlation between residence time and ozone above, it is justified to consider that air masses resident over the Northern Indian Subcontinent for 4–6 days represent regionally polluted air over this region. Therefore, ozone levels associated with 4–6 days residence time of air masses and median altitude of less than 4000 m over the Northern Indian Subcontinent are classified as "regionally polluted ozone" following the method of *Naja et al.* [2003a]. Figure 8 shows seasonal variations in regionally polluted ozone with maximum levels in spring and minimum in summer/monsoon. The annual mean value of ozone in regionally polluted air masses is 47.1 ± 16.7 ppbv.

[31] The influence of air masses from the marine region over the central Himalayas is also studied (Figure 8). Such air masses reach Nainital only during June, July and August. The average residence time of these air masses over the marine region is 2.3 ± 1.6 days and the median altitude is 616 m over the Northern Indian Subcontinent which means that these air masses generally travel at lower altitude and therefore some continental influence cannot be ruled out. Therefore, air masses with a residence time of more than three days over the marine region and with a median altitude greater than 1100 m over the Northern Indian Subcontinent are classified as "marine" air masses to reduce the influence of continental emissions. The estimated average ozone in these marine air masses is 29.7 ± 11.9 ppbv during June–August 2007–08. Interestingly, these estimates of ozone in marine air masses are reasonably comparable with summer/monsoon time background ozone (34.7 ppbv) estimates made using zero day extrapolation methods. Additionally, these ozone levels are also similar to the background ozone estimated over western Indian region [*Naja et al.*, 2003b].

[32] To identify the influences of long-range transport from Africa/Europe (defined in section 3.2), the residence time of air masses are also estimated over this region. If the residence time over Africa/Europe is more than 4 days and the median altitude of trajectories is greater than 4000 m over the Northern Indian Subcontinent, then such air masses are classified as Africa/Europe air masses. Here, the altitude of more than 4000 m over the Northern Indian Subcontinent is considered to minimize the influence from regional pollution of Indian region so that contributions from Africa/Europe region remain significant in these air masses. However, the higher altitude of trajectories analyzed here suggests

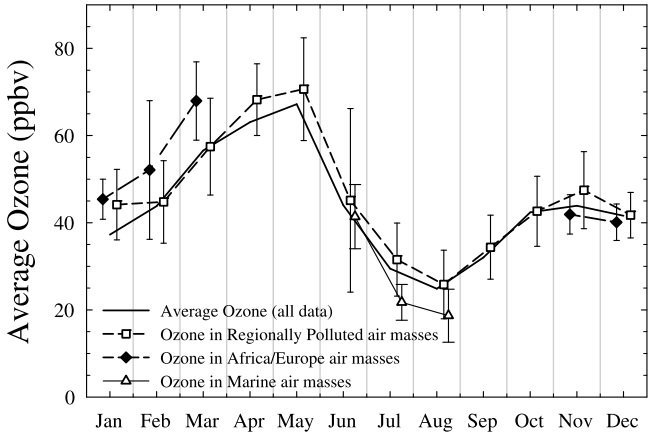

Figure 8. Variations in average ozone mixing ratios in all data, regionally polluted air masses, Africa/Europe air masses, and marine air masses during October 2006 to December 2008. Vertical bars denote the one sigma variation in the corresponding ozone averages.

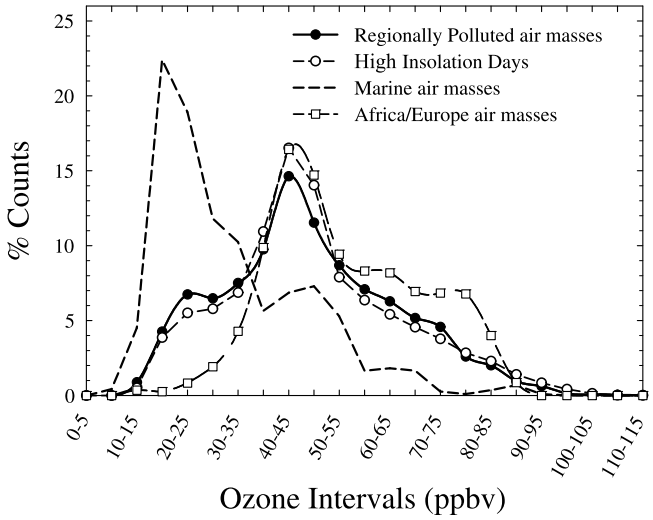

Figure 9. Frequency analyses of ozone associated with regionally polluted, marine, and Africa/Europe air masses during October 2006 to December 2008. The frequency analysis for ozone associated with high insolation days is also shown. Ozone associated with high insolation days, regionally polluted air masses and Africa/Europe air masses show maximum contributions in the interval 40–45 ppbv, while the region of maximum contribution in ozone data associated with marine air masses is in the lower ozone interval of 15–20 ppbv.

that there may also be a larger contribution from stratospheric sources in these air masses. Seasonal variation in ozone associated with these air masses is shown in Figure 8. The influence of long range transport (altitude > 4000 m) from the western sector encompassing the Africa/Europe region is seen from November to March with greatest influence during January–March. The contribution from this region is as high as 11.3 ppbv in March. The average ozone mixing ratio during January to March in these air masses (Africa/Europe > 4000m) is 57.7 ± 15.4 ppbv, while the average of all ozone data during January–March is 47.5 ± 15.9 ppbv. Trajectory based analysis indicates that up to 40% of the tropospheric air entering east Asia may be influenced by European sources [*Newell and Evans*, 2000], and previous model studies have suggested that European sources may contribute about 4 ppbv of ozone over Central Asia in spring [*Wild et al.*, 2004].

4.4.3. Frequency Analyses

[33] Frequency analyses for ozone associated with different air masses during October 2006 to December 2008 are shown in Figure 9. As expected, ozone distributions in regionally polluted and Africa/Europe air masses show high ozone much more frequently than marine air masses. Maximum contribution to the ozone distributions in regionally polluted (14.6%) and Africa/Europe (16.4%) air masses is from ozone between 40 and 45 ppbv while it is from 15 to 20 ppbv for marine air masses. Figure 9 also shows the frequency analysis for ozone associated with high insolation days, and this is in good agreement with that for regionally polluted air masses.

[34] Note that the contribution from higher ozone values (greater than 60 ppbv) is larger for Africa/Europe air masses than for other air masses. This suggests that long-range transport from Africa/Europe, along with the greater influence from stratospheric sources associated with higher altitude transport, can play a crucial role in influencing regional atmospheric composition and air quality over the central Himalayas.

4.5. Comparison With Model Data

[35] Figure 10 shows a comparison of FRSGC/UCI model results with ozone observations at Nainital. Modeled ozone is shown for both the model surface layer at Nainital (1600 m) and for a pressure altitude equivalent to about 2000 m. Differences between simulated and observed ozone values are evident. The model shows an increase from winter to spring with lower levels in the summer/monsoon period, but there are large differences in ozone abundance, particularly during spring and summer/monsoon. The model results in summer are likely to be biased by strong anthropogenic emissions on the plain and since Nainital is located on the edge of the mountains, the model is not able to resolve the differing chemical and meteorological environments cleanly. The complex topography in this region and coarse resolution emission data may also contribute to the poor representation of ozone at the Nainital site. Interestingly, model results in the surface layer are in better agreement in winter. The contribution of stratospheric ozone is derived from the model using an ozone tracer of stratospheric origin following *Roelofs and Lelieveld* [1997], and the contribution of anthropogenic precursor emissions from European and South Asian sources are derived from separate model simulations with reduced emissions over these regions. These results are also shown in Figure 10b. Contribution from South Asian sources, dominated by Indian emissions, is greatest (9–10 ppbv) in summer/monsoon even though the overall ozone abundance and

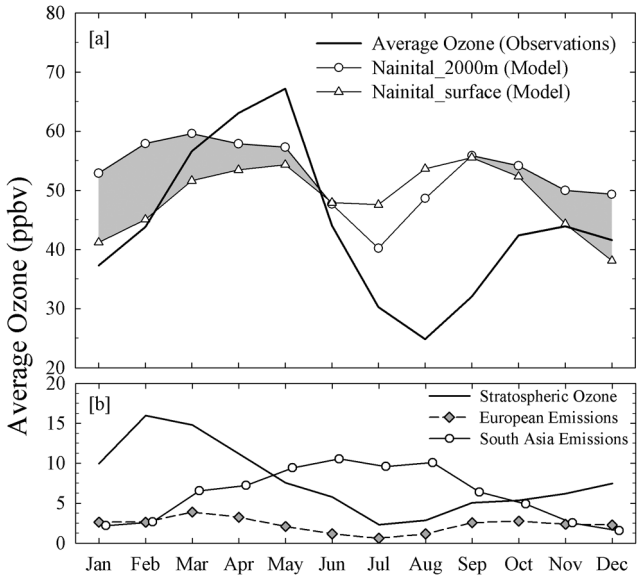

Figure 10. Comparison of ozone observations at Nainital with the model simulations. Model simulations are made with the meteorological data of 2001. Contributions of stratospheric ozone, European emissions and South Asia emissions, derived from the model, are also shown.

Table 2. Seasonal Average and One Sigma Deviation for Ozone Associated With Air Masses When the Median Altitude of the Corresponding Trajectory Is Above 4000 m During October 2006 to December 2008[a]

Season	Trajectories From Above 4000 m (%)	Ozone[b] (ppbv)	RH[b] (%)
Winter (DJF)	10.3	43.1 ± 11.9	52.6 ± 26.2
Spring (MAM)	14.9	66.9 ± 12.5	50.0 ± 22.0
Summer/monsoon(JJA)	0	-	-
Autumn (SON)	15.3	42.0 ± 6.1	71.6 ± 19.5

[a]The percentage of such trajectories in each season is also shown.
[b]Mean ± 1 Sigma.

lifetime is a minimum in this season. This reflects the dominance of the prevailing transport patterns over the effects of local photochemistry. Interestingly, the modeled ozone build-up due to South Asian emissions in spring is in reasonable agreement with the observed spring build-up derived from the insolation characterization (Figure 6). Influence of European emissions is 2–4 ppbv and is greatest in March, also reflecting the prevailing transport patterns.

[36] The stratospheric contribution lies between 2 and 16 ppbv, with more than 10 ppbv during January–April. While the contribution of stratospheric sources to surface ozone has been found to be small in some observational studies [e.g., *Dibb et al.*, 1994; *Derwent et al.*, 1998], it has been shown to be substantial at some locations, particularly at higher-altitude mountain sites such as this [e.g., *Tsutsumi et al.*, 1998; *Langford et al.*, 2009].

[37] We have also attempted to identify the influence of downward transport using back air trajectories. Observed ozone values at Nainital are characterized along trajectories of median altitude greater than 4000 m. Such trajectories have a smaller influence from surface emissions and represent air masses from higher altitudes. Table 2 shows seasonal average ozone levels associated with these air masses. It can be noted that there are no trajectories arriving from these higher altitudes in the summer/monsoon. To get further insight into the sources of these air masses, we use relative humidity data, since sinking air masses are characterized by lower relative humidity. It is evident that air masses from above 4000 m are drier during winter and spring than during autumn (Table 2). Ozone levels associated with air masses with median altitudes more than 4000 m are highest in spring (66.9 ± 12.5 ppbv) and they are about 4.6 ppbv higher than those in regionally polluted air masses during spring. This is similar to the difference in stratospheric ozone contributions between the two altitudes considered in the model, about 4–6 ppbv in spring. These are only first-order estimates and further analysis is required for better quantification of the contribution from downward transport.

5. Discussion and Conclusions

[38] Surface ozone measurements have been made for the first time at Nainital, a high-altitude site in the central Himalayas, from October 2006 to December 2008. Diurnal variations do not show significant in situ photochemical build-up of ozone at this site. Ozone levels clearly show a spring maximum with highest monthly average values in May while lowest ozone levels are observed during the summer/monsoon season. Solar radiation, rainfall, backward trajectories, fire counts and simulations with a chemical transport model are used to investigate the different processes contributing to the seasonal variation in ozone at Nainital. Annual average ozone values on high and low insolation days estimated using daytime solar radiation data are 46.8 ppbv and 39.9 ppbv respectively. Spatial and temporal classification of air masses was used to derive ozone in regionally polluted, marine and Africa/Europe air masses. Based on correlating the increase in ozone with the residence time of air masses over the Northern Indian Subcontinent, the ozone growth rate was estimated to average 3.2 ppbv per day for up to 6 days in spring. Similar growth rates in ozone have been observed over central Europe [*Naja et al.*, 2003a].

[39] Annual average regionally polluted ozone levels (47.1 ppbv) estimated using the ozone associated with 4–6 day residence times over the Northern Indian Subcontinent agree reasonably well with those on days with high insolation (46.8 ppbv) and are about 7 ppbv higher than those on days with low insolation during the observation period. The build-up in ozone levels is as high as 16.5 ppbv in May–June. It is shown that observed solar radiation and rainfall at Nainital are representative of the Northern Indian Subcontinent and it is also seen that in situ ozone production close to the site plays a negligible role. Therefore, it is suggested that this build-up of 16.5 ppbv could be representative of the Northern Indian Subcontinent. The stratospheric ozone contribution derived from the model is greater than 10 ppbv during January–April. Interestingly, trajectory assisted analysis shows that the contribution to springtime ozone from higher altitudes (>4000 m) is about 4.6 ppbv higher than that in regionally polluted air masses, which is in agreement with model-derived values.

[40] Estimates of ozone in marine air masses are shown to be reasonably comparable with summer/monsoon time background ozone estimates that are in the range of 30–35 ppbv. The contribution of long-range transport is greatest in January–March at about 8–11 ppbv. It is seen that coupling spatial classification and residence time classification of air masses with solar radiation provides a more useful characterization of ozone than either method alone.

[41] The model used here is not capable of reproducing the strength of the seasonal variation at Nainital. This is probably due to the sharp changes in topography along the edge of the Himalayan region and the coarse spatial resolution of model, and may also reflect weaknesses in the emission data. There have been few global chemical transport model studies of the South Asian region. A modeling study by *Engardt* [2008] indicates discrepancies between modeled and observed ozone values over India, particularly in the summer/monsoon period. Regional models also show limitations in reproducing observed values over South Asia [*Mittal et al.*, 2007; *Roy et al.*, 2008]. Additionally, great uncertainty lies in emissions estimates over Asia [*Streets et al.*, 2003, 2006; *Akimoto et al.*, 2006] and there is a mismatch in satellite-based observations with emission estimates [*Akimoto et al.*, 2006].

[42] This work highlights differences in the seasonal variation of surface ozone over two regions in India: the central Himalayan region and the western part of India. Ozone

levels at Nainital are found to be 24–29 ppbv higher than those seen in Western India (Mt. Abu, 1680 m amsl) during April and May. Lower values at Mt. Abu are largely due to the lower influence of emissions from the Indo-Gangetic Plain (IGP) region in the western part of India and the arrival of pristine marine air masses at this site during spring [*Naja et al.*, 2003b]. Air masses arriving at Mt. Abu have a shorter residence time (~2 days) over the Northern Indian Subcontinent (including the IGP region) compared to those arriving at Nainital (~5 days).

[43] The only available study of ozone with yearlong observations over the Himalayan region indicates higher ozone in spring [*Pudasainee et al.*, 2006]. However, these data may not be regionally representative as these observations are made at an urban site in the Kathmandu valley. Ozone is 4–12 ppbv higher at Nainital than at other global high-altitude sites like Mauna Loa (3397 m amsl) and Mt. Fuji (3776 m amsl) [*Oltmans et al.*, 2006]. Such higher ozone at Nainital suggests that regional pollution, particularly from the Indo-Gangetic Plain (IGP), leads to enhancement in ozone over the central Himalayas. The tropospheric ozone column over this region has also been shown to be high in earlier satellite based studies [*Fishman et al.*, 2003].

[44] We feel that this high-altitude site at Nainital is more regionally representative of the northern part of India. We conclude that seasonal variations in ozone at Nainital are largely controlled by regional pollution in the Northern Indian Subcontinent with some contributions from biomass burning, downward transport and long range transport with en-route chemical transformation. Different studies on the influence of European outflow to East Asia suggest that the Siberian anticyclone promotes transport of European air masses to East Asia at relatively low altitudes [e.g., *Newell and Evans*, 2000; *Liu et al.*, 2002]. However, the influence of Africa/Europe outflow over south Asia is not well studied and might contribute to higher ozone in winter and early spring. This work suggests that Nainital observation site is an excellent place for monitoring the flow of oxidants into the Himalayas, and for further future analysis of stratospheric influence, how it interacts with anthropogenic pollution, and the role that mountain and monsoon systems play in affecting outflow from India.

[45] **Acknowledgments.** We are grateful to Shyam Lal, Ram Sagar, and C.B.S. Dutt for fruitful discussions and for their keen interest and support for this program. We thank Jiye Zeng (NIES, Tsukuba) for providing the METEX model. Fire count data have been obtained from http://dup.esrin.esa.int/ionia/wfa/index.asp. The NCEP Reanalysis data is provided by the NOAA/OAR/ESRL PSD, Boulder, Colorado, from their Web site at http://www.cdc.noaa.gov/. The TRMM rainfall data used in this study were acquired using the GES-DISC Interactive Online Visualization and Analysis Infrastructure (Giovanni) as part of the NASA's Goddard Earth Science (GES) Data and Information Services Center (DISC). Suggestions and comments from three anonymous reviewers are greatly appreciated.

References

Akimoto, H. (2003), Global air quality and pollution, *Science*, *302*, 1716–1719, doi:10.1126/science.1092666.

Akimoto, H., T. Ohara, J. Kurokawa, and N. Horri (2006), Verification of energy consumption in China during 1996–2003 by using satellite observational data, *Atmos. Environ.*, *40*, 7663–7667, doi:10.1016/j.atmosenv.2006.07.052.

Aneja, V. P., et al. (2001), Measurements and analysis of criteria pollutants in New Delhi, India, *Environ. Int.*, *27*, 35–42, doi:10.1016/S0160-4120(01)00051-4.

Asnani, G. C. (2005), Climatology of the tropics, in *Tropical Meteorology*, vol. 1, pp. 100–204, G.C. Asnani, Pune, India.

Beig, G., S. Gunthe, and D. B. Jadhav (2007), Simultaneous measurements of ozone and its precursors on a diurnal scale at a semi urban site in India, *J. Atmos. Chem.*, *57*, 239–253, doi:10.1007/s10874-007-9068-8.

Carver, G. D., P. D. Brown, and O. Wild (1997), The ASAD atmospheric chemistry integration package and chemical reaction database, *Comput. Phys. Commun.*, *105*, 197–215, doi:10.1016/S0010-4655(97)00056-8.

Derwent, R. G., P. G. Simmonds, S. Seuring, and C. Dimmer (1998), Observation and interpretation of the seasonal cycles in the surface concentrations of ozone and carbon monoxide at Mace Head, Ireland from 1990 to 1994, *Atmos. Environ.*, *32*, 145–157, doi:10.1016/S1352-2310(97)00338-5.

Desqueyroux, H., J. C. Pujet, M. Prosper, F. Squinazi, and I. Momas (2002), Short-term effects of low-level air pollution on respiratory health of adults suffering from moderate to severe asthma, *Environ. Res.*, *89*, 29–37, doi:10.1006/enrs.2002.4357.

Dibb, J. E., L. D. Macker, R. C. Finkel, J. R. Southon, M. W. Caffee, and L. A. Barrie (1994), Estimation of the stratospheric input to the Arctic troposphere: ^{7}Be and ^{10}Be in aerosols at Alert, Canada, *J. Geophys. Res.*, *99*, 12,855–12,864, doi:10.1029/94JD00742.

Dickerson, R. R., et al. (2007), Aircraft observations of dust and pollutants over northeast China: Insight into the meteorological mechanism of transport, *J. Geophys. Res.*, *112*, D24S90, doi:10.1029/2007JD008999.

Di Girolamo, L., et al. (2004), Analysis of Multi-angle Imaging Spectro-Radiometer (MISR) aerosol optical depths over greater India during winter 2001–2004, *Geophys. Res. Lett.*, *31*, L23115, doi:10.1029/2004GL021273.

Ding, A., and T. Wang (2006), Influence of stratosphere-to-troposphere exchange on the seasonal cycle of surface ozone at Mount Waliguan in western China, *Geophys. Res. Lett.*, *33*, L03803, doi:10.1029/2005GL024760.

Ding, A. J., et al. (2008), Tropospheric ozone climatology over Beijing: Analysis of aircraft data from the MOZAIC program, *Atmos. Chem. Phys.*, *8*, 1–13, doi:10.5194/acp-8-1-2008.

Engardt, M. (2008), Modelling of near-surface ozone over South Asia, *J. Atmos. Chem.*, *59*, 61–80, doi:10.1007/s10874-008-9096-z.

Fiore, A. M., et al. (2009), Multimodel estimates of intercontinental source-receptor relationships for ozone pollution, *J. Geophys. Res.*, *114*, D04301, doi:10.1029/2008JD010816.

Fishman, J., A. E. Wozniak, and J. K. Creilson (2003), Global distribution of tropospheric ozone from satellite measurements using the empirically corrected tropospheric ozone residual technique: Identification of the regional aspects of air pollution, *Atmos. Chem. Phys.*, *3*, 893–907, doi:10.5194/acp-3-893-2003.

Jain, S. L., B. C. Arya, A. Kumar, S. D. Ghude, and P. S. Kulkarni (2005), Observational study of surface ozone at New Delhi, India, *Int. J. Remote Sens.*, *26*(16), 3515–3524, doi:10.1080/01431160500076616.

Jethva, H., S. K. Satheesh, and J. Srinivasan (2005), Seasonal variability of aerosols over the Indo-Gangetic basin, *J. Geophys. Res.*, *110*, D21204, doi:10.1029/2005JD005938.

Kalnay, E., et al. (1996), The NCEP/NCAR 40-Year Reanalysis Project, *Bull. Am. Meteorol. Soc.*, *77*, 437–471, doi:10.1175/1520-0477(1996)077<0437:TNYRP>2.0.CO;2.

Kaufman, Y. J., et al. (1998), Potential global fire monitoring from EOS-MODIS, *J. Geophys. Res.*, *103*, 32,215–32,238, doi:10.1029/98JD01644.

Kleinman, L., et al. (1994), Ozone formation at a rural site in the southern United States, *J. Geophys. Res.*, *99*, 3469–3482, doi:10.1029/93JD02991.

Lal, S., M. Naja, and B. H. Subbaraya (2000), Seasonal variations in surface ozone and its precursors over an urban site in India, *Atmos. Environ.*, *34*, 2713–2724, doi:10.1016/S1352-2310(99)00510-5.

Langford, A. O., K. C. Aikin, C. S. Eubank, and E. J. Williams (2009), Stratospheric contribution to high surface ozone in Colorado during springtime, *Geophys. Res. Lett.*, *36*, L12801, doi:10.1029/2009GL038367.

Lin, X., M. Trainer, and S. C. Liu (1988), On the nonlinearity of the tropospheric ozone production, *J. Geophys. Res.*, *90*, 3753–3772.

Liu, H., D. J. Jacob, L. Y. Chan, S. J. Oltmans, I. Bey, R. M. Yantosca, J. M. Harris, B. N. Duncan, and R. V. Martin (2002), Sources of tropospheric ozone along the Asian Pacific Rim: An analysis of ozonesonde observations, *J. Geophys. Res.*, *107*(D21), 4573, doi:10.1029/2001JD002005.

Logan, A. Z. (1985), Tropospheric ozone: Seasonal behavior, trends, and anthropogenic influence, *J. Geophys. Res.*, *90*, 10,463–10,482, doi:10.1029/JD090iD06p10463.

Ma, J., X. Zheng, and X. Xu (2005), Comment on "Why does surface ozone peak in summertime at Waliguan?" by Bin Zhu et al., *Geophys. Res. Lett.*, *32*, L01805, doi:10.1029/2004GL021683.

Mauzerall, D. L., and X. P. Wang (2001), Protecting agricultural crops from the effects of tropospheric ozone exposure: Reconciling science and standard setting in the United States, Europe, and Asia, *Annu. Rev. Energy Environ.*, *26*, 237–268, doi:10.1146/annurev.energy.26.1.237.

Mittal, M. L., P. G. Hess, S. L. Jain, B. C. Arya, and C. Sharma (2007), Surface ozone in the Indian region, *Atmos. Environ.*, *41*, 6572–6584, doi:10.1016/j.atmosenv.2007.04.035.

Nair, P. R., et al. (2002), Temporal variations in surface ozone at Thumba (8.6°N, 77°E): A tropical coastal site in India, *Atmos. Environ.*, *36*, 603–610, doi:10.1016/S1352-2310(01)00527-1.

Naja, M., and S. Lal (2002), Surface ozone and precursor gases at Gadanki (13.5° N, 79.2° E), tropical rural site in India, *J. Geophys. Res.*, *107*(D14), 4197, doi:10.1029/2001JD000357.

Naja, M., H. Akimoto, and J. Staehelin (2003a), Ozone in background and photochemically aged air over central Europe: Analysis of long-term ozonesonde data from Hohenpeissenberg and Payrene, *J. Geophys. Res.*, *108*(D2), 4063, doi:10.1029/2002JD002477.

Naja, M., S. Lal, and D. Chand (2003b), Diurnal and seasonal variabilities in surface ozone at a high-altitude site Mt. Abu (24.6°N, 72.7°E, 1680 m asl) in India, *Atmos. Environ.*, *37*, 4205–4215, doi:10.1016/S1352-2310(03)00565-X.

Newell, R. E., and M. J. Evans (2000), Seasonal changes in pollutant transport to the North Pacific: The relative importance of Asian and European sources, *Geophys. Res. Lett.*, *27*, 2509–2512, doi:10.1029/2000GL011501.

Niranjan, K., V. Sreekanth, B. L. Madhavan, and K. Krishna Moorthy (2006), Wintertime aerosol characteristics at a north Indian site Kharagpur in the Indo-Gangetic plains located at the outflow region into Bay of Bengal, *J. Geophys. Res.*, *111*, D24209, doi:10.1029/2006JD007635.

Ohara, T., H. Akimoto, J. Kurokawa, N. Horri, K. Yamaji, X. Yan, and T. Hayasaka (2007), An Asian emission inventory of anthropogenic emission sources for the period 1980–2020, *Atmos. Chem. Phys.*, *7*, 4419–4444, doi:10.5194/acp-7-4419-2007.

Oksanen, E., and T. Holopainen (2001), Responses of two birch (Betula pendula Roth) clones to different ozone profiles with similar AOT40 exposure, *Atmos. Environ.*, *35*, 5245–5254, doi:10.1016/S1352-2310(01)00346-6.

Oltmans, S. J., and H. Levy II (1994), Surface ozone measurements from a global network, *Atmos. Environ.*, *28*, 9–24, doi:10.1016/1352-2310(94)90019-1.

Oltmans, S. J., et al. (2006), Long-term changes in tropospheric ozone, *Atmos. Environ.*, *40*, 3156–3173, doi:10.1016/j.atmosenv.2006.01.029.

Panday, A. K., and R. G. Prinn (2009), The diurnal cycle of air pollution in the Kathmandu Valley, Nepal: Part 1: Observations, *J. Geophys. Res.*, *114*, D09305, doi:10.1029/2008JD009777.

Pant, P., et al. (2006), Aerosol characteristics at a high-altitude location in central Himalayas, *J. Geophys. Res.*, *111*, D17206, doi:10.1029/2005JD006768.

Pochanart, P., H. Akimoto, S. Maksyutov, and J. Staehelin (2001), Surface ozone at the Swiss Alpine site Arosa: The hemispheric background and the influence of large-scale anthropogenic emissions, *Atmos. Environ.*, *35*, 5553–5566, doi:10.1016/S1352-2310(01)00236-9.

Pudasainee, D., et al. (2006), Ground level ozone concentrations and its association with NO_x and meteorological parameters in Kathmandu valley, Nepal, *Atmos. Environ.*, *40*, 8081–8087, doi:10.1016/j.atmosenv.2006.07.011.

Roelofs, G. J., and J. Lelieveld (1997), Model study of the influence of cross-tropopause O_3 transports on tropospheric O_3 levels, *Tellus, Ser. B*, *49*, 38–55, doi:10.1034/j.1600-0889.49.issue1.3.x.

Roy, S., G. Beig, and D. Jacob (2008), Seasonal distribution of ozone and its precursors over the tropical Indian region using regional chemistry-transport model, *J. Geophys. Res.*, *113*, D21307, doi:10.1029/2007JD009712.

Sagar, R., B. Kumar, U. C. Dumka, K. Krishna Moorthy, and P. Pant (2004), Characteristics of aerosol optical depths over Manora Peak: A high-altitude station in the central Himalayas, *J. Geophys. Res.*, *109*, D06207, doi:10.1029/2003JD003954.

Solberg, S., et al. (2008), European surface ozone in extreme summer 2003, *J. Geophys. Res.*, *113*, D07307, doi:10.1029/2007JD009098.

Staehelin, J., J. Thudium, R. Buehlfr, and A. Volz-Thomas (1994), Trends in surface ozone concentrations at Arosa (Switzerland), *Atmos. Environ.*, *28*, 75–87, doi:10.1016/1352-2310(94)90024-8.

Stevenson, D. S., et al. (2006), Multimodel ensemble simulations of present-day and near-future tropospheric ozone, *J. Geophys. Res.*, *111*, D08301, doi:10.1029/2005JD006338.

Streets, D. G., and S. T. Waldhoff (2000), Present and future emissions of air pollutants in China: SO_2, NO_x and CO, *Atmos. Environ.*, *34*, 363–374, doi:10.1016/S1352-2310(99)00167-3.

Streets, D. G., et al. (2003), An inventory of gaseous and primary aerosol emissions in Asia in the year 2000, *J. Geophys. Res.*, *108*(D21), 8809, doi:10.1029/2002JD003093.

Streets, D. G., et al. (2006), Revisiting China's CO emissions after the Transport and Chemical Evolution over the Pacific (TRACE-P) mission: Synthesis of inventories, atmospheric modeling and observations, *J. Geophys. Res.*, *111*, D14306, doi:10.1029/2006JD007118.

Tang, J., et al. (1995), Surface ozone measurement at China GAW baseline observatory, paper presented at the Conference on the Measurement and Assessment of Atmospheric Composition Change, World Meteorol. Organ., Int. Global Atoms. Chem., Beijing.

Tanimoto, H. (2009), Increase in springtime tropospheric ozone at a mountainous site in Japan for the period 1998–2006, *Atmos. Environ.*, *43*, 1358–1363, doi:10.1016/j.atmosenv.2008.12.006.

Tripathi, S. N., S. Dey, V. Tare, and S. K. Satheesh (2005), Aerosol black carbon radiative forcing at an industrial city in Northern India, *Geophys. Res. Lett.*, *32*, L08802, doi:10.1029/2005GL022515.

Tsutsumi, Y., Y. Zaizen, and Y. Makino (1994), Tropospheric ozone measurement at the top of Mt. Fuji, *Geophys. Res. Lett.*, *21*, 1727–1730, doi:10.1029/94GL01107.

Tsutsumi, Y., Y. Igarashi, Y. Zaizen, and Y. Makino (1998), Case studies of tropospheric ozone events observed at the summit of Mount Fuji, *J. Geophys. Res.*, *103*, 16,935–16,951, doi:10.1029/98JD01152.

van der Werf, G. R., T. J. Randerson, J. Collatz, and L. Giglio (2003), Carbon emissions from fires in tropical and subtropical ecosystems, *Global Change Biol.*, *9*, 547–562, doi:10.1046/j.1365-2486.2003.00604.x.

Wang, T., et al. (2009), Increasing surface ozone concentrations in the background atmosphere of southern China 1994–2007, *Atmos. Chem. Phys.*, *9*, 6217–6227, doi:10.5194/acp-9-6217-2009.

Wild, O., and M. J. Prather (2000), Excitation of the primary tropospheric chemical mode in a global 3-D model, *J. Geophys. Res.*, *105*, 24,647–24,660.

Wild, O., P. Pochanart, and H. Akimoto (2004), Trans-Eurasian transport of ozone and its precursors, *J. Geophys. Res.*, *109*, D11302, doi:10.1029/2003JD004501.

Xu, X., et al. (2008), Long-term trend of surface ozone at a regional background station in eastern China 1991–2006: Enhanced variability, *Atmos. Chem. Phys.*, *8*, 2595–2607, doi:10.5194/acp-8-2595-2008.

Zeng, J., Y. Tohjima, Y. Fujinuma, H. Mukai, and M. Katsumoto (2003), A study of trajectory quality using methane measurements from Hateruma Isaland, *Atmos. Environ.*, *37*, 1911–1919, doi:10.1016/S1352-2310(03)00048-7.

Zheng, X. D., G. J. Wang, J. Tang, X. C. Zhang, W. Yang, H. N. Lee, and C. S. Wang (2005), Be-7 and Pb-210 radioactivity and implications on sources of surface ozone at Mt. Waliguan, *Chin. Sci. Bull.*, *50*(2), 167–171.

Zhu, B., et al. (2004), Why does surface ozone peak in summertime at Waliguan?, *Geophys. Res. Lett.*, *31*, L17104, doi:10.1029/2004GL020609.

R. Kumar and M. Naja, Aryabhatta Research Institute of Observational Sciences, Manora Peak, Nainital 263129, India. (manish@aries.res.in)

S. Venkataramani, Physical Research Laboratory, Navrangpura, Ahmedabad 380009, India.

O. Wild, Lancaster Environment Centre, Lancaster University, Lancaster LA1 4YQ, UK.